Electronic Supplementary Material (ESI) for Physical Chemistry Chemical Physics.

Supplemental Materials

Table of Contents

Effects of Spin-Orbit Coupling

In order to investigate the impact of the heavy-atom effect on the calculated reaction path, spin-orbit coupling (SOC) has been calculated as a correction to the ground state energy. These corrections, derived from single-point calculations using the ORCA 5.0.3 quantum chemistry program[1], are presented in Table S1. For this purpose, an all-electron approach was necessary as opposed to the use of effective core potential to describe the core-electron of the heavy-atoms.

In the calculation, the PBE0 hybrid functional[2] and D3(BJ) dispersion correction[3,4] were employed. The scalar relativistic effects were accounted for using the zeroth-order regular approximation[5,6] (ZORA) and the relativistically recontracted ZORA-TZVP basis set[7] was applied to hydrogen, boron and carbon atoms. The segmented all-electron relativistically contracted SARC-ZORA-TZVP basis set[8,9] was applied to zirconium and hafnium centers. The structures were not re-optimized. Ten singlet and ten triplet excited states were calculated with linear-response time-dependent density functional theory[10] (LR-TDDFT) using the closed-shell ground state as the reference state. The spin-orbit coupling operator was calculated by the SOMF-(1X)[11] approach implemented in ORCA. The RIJCOSX algorithm was used throughout to accelerate the calculations.

It was observed that the spin-orbit coupling was trivial to the reaction path. Despite some inconsistencies arising from the use of a different method and the fact that the geometries were not re-optimized, it is reasonable to conclude that the inclusion of spin-orbit coupling does not significantly alter the favored reaction paths identified in the main text.

SOC correction	cm^{-1}	$kcal \cdot mol^{-1}$
CpHf-1a	-7.7	-0.022
CpHf-1a-TS-2a	-19.4	-0.055
CpHf-1b	-45.6	-0.130
CpHf-2a	-40.0	-0.114
CpHf-2a-TS-2f	-69.7	-0.199
CpZr-1a	-0.6	-0.002
CpZr-1a-TS-2a	-1.2	-0.003
CpZr-1b	-2.9	-0.008
CpZr-2a	-2.6	-0.007
CpZr-2a-TS-2f	-3.9	-0.011

SOC correction	cm^{-1}	$kcal \cdot mol^{-1}$
CpZr-2a-TS-3a	-3.1	-0.009
CpZr-2f	-1.0	-0.003
CpZr-3a	-4.6	-0.013
Hf-1a	-0.2	-0.001
Hf-1a-TS-2a	-23.3	-0.067
Hf-1b	-53.7	-0.153
Hf-2a	-44.6	-0.127
Hf-2a-TS-2f	-47.3	-0.135
Hf-2a-TS-3a	-76.3	-0.218
Hf-2f	-13.5	-0.039

SOC correction	cm^{-1}	$kcal \cdot mol^{-1}$
Hf-3a	-104.3	-0.298
Zr-1a	0.0	0.000
Zr-1a-TS-2a	-1.7	-0.005
Zr-1b	-3.4	-0.010
Zr-2a	-2.8	-0.008

SOC correction	cm^{-1}	$kcal \cdot mol^{-1}$
Zr-2a-TS-2f	-3.4	-0.010
Zr-2a-TS-3a	-4.5	-0.013
Zr-2f	-1.0	-0.003
Zr-3a	-5.6	-0.016

Table S1. Spin orbit coupling corrections to the ground state energy of selected geometries.

References

1 F. Neese, F. Wennmohs, U. Becker and C. Riplinger, *J Chem Phys*, 2020, **152**, 224108.

2 C. Adamo and V. Barone, *J Chem Phys*, 1999, **110**, 6158–6170.

3 S. Grimme, J. Antony, S. Ehrlich and H. Krieg, *J Chem Phys*, 2010, **132**, 154104.

4 S. Grimme, S. Ehrlich and L. Goerigk, *J Comput Chem*, 2011, **32**, 1456–1465.

5 E. van Lenthe, E. J. Baerends and J. G. Snijders, *J Chem Phys*, 1993, **99**, 4597–4610.

6 C. van Wüllen, *J Chem Phys*, 1998, **109**, 392–399.

7 A. Canal Neto, I. B. Ferreira, F. E. Jorge and A. Z. de Oliveira, *Chem Phys Lett*, 2021, **771**, 138548.

8 D. A. Pantazis, X.-Y. Chen, C. R. Landis and F. Neese, *J Chem Theory Comput*, 2008, **4**, 908–919.

9 J. D. Rolfes, F. Neese and D. A. Pantazis, *J Comput Chem*, 2020, **41**, 1842–1849.

10 R. Bauernschmitt and R. Ahlrichs, *Chem Phys Lett*, 1996, **256**, 454–464.

11 F. Neese, *J Chem Phys*, 2005, **122,** 034107.

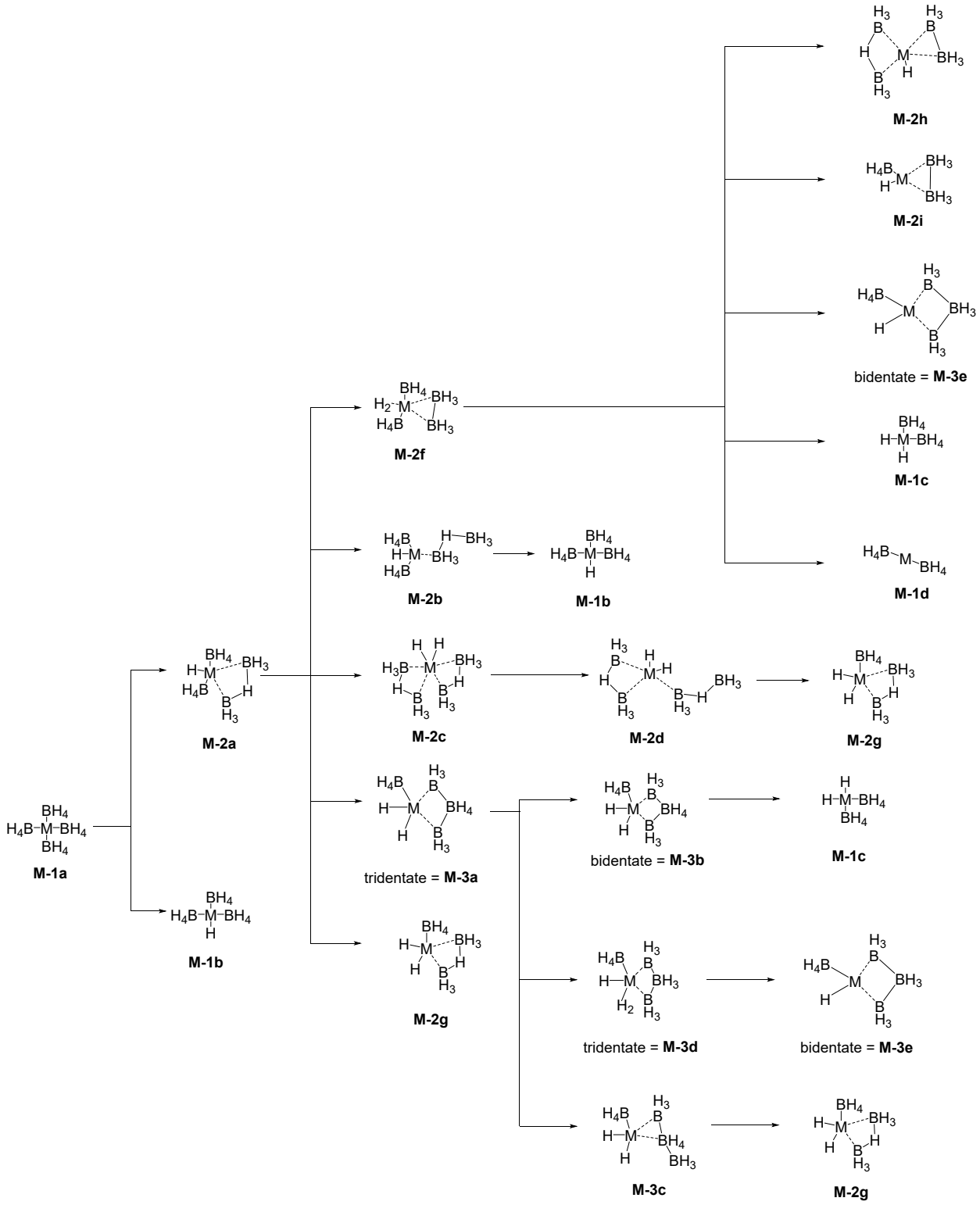

Figure S1: Reaction map of the tetrakis complex. M = Zr, Hf.

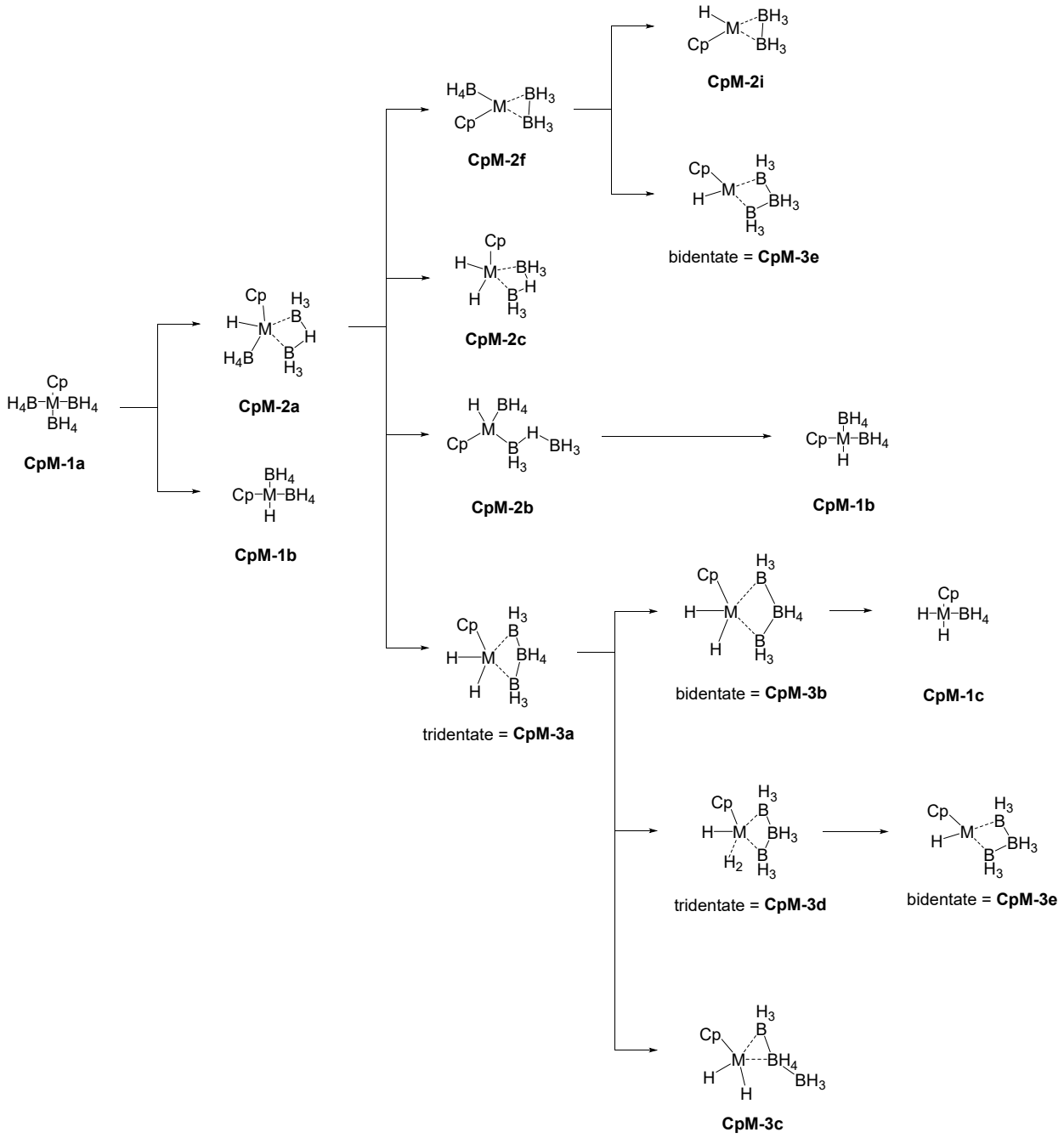

Figure S2: Reaction map of the cyclopentadienyl complex. M = Zr, Hf.

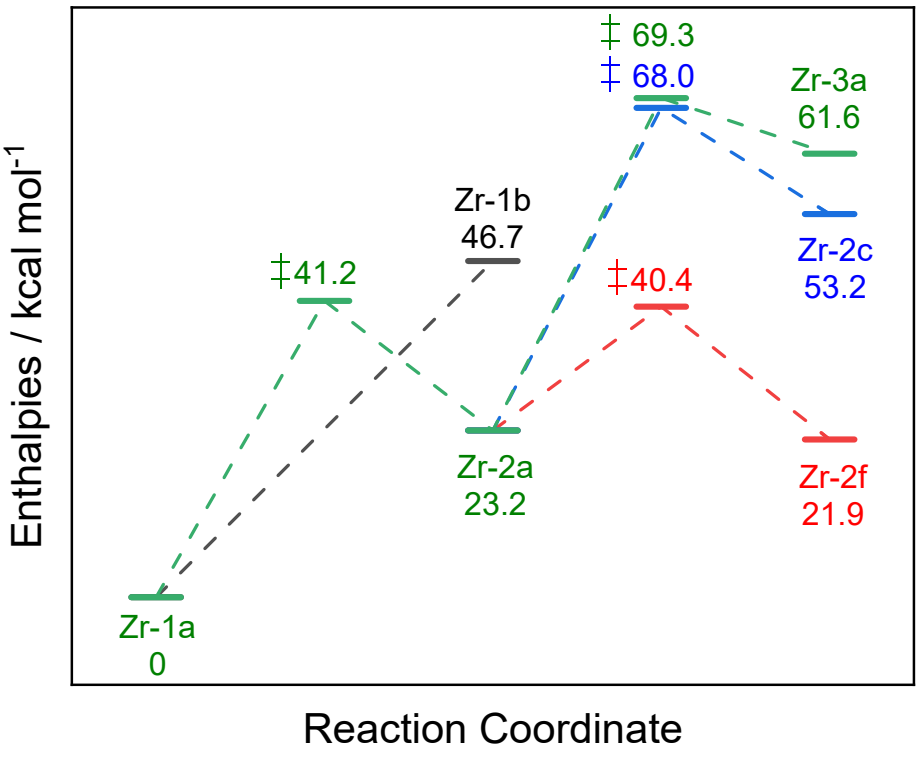

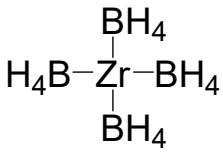

Zr-1a

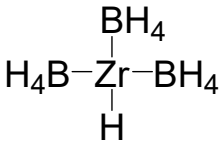

Zr-1b

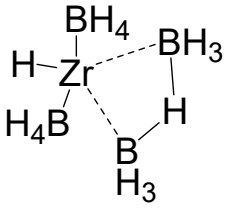

Zr-2a

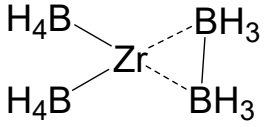

Zr-2f

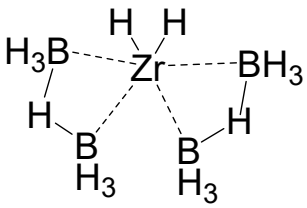

Zr-2c

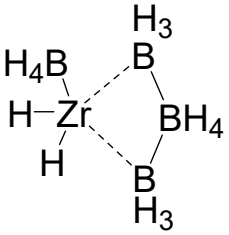

tridentate = **Zr-3a**

Figure S3: Reaction coordinate diagram of the initial reactions of all $Zr(BH_4)_4$ pathways. All enthalpies were calculated at 298.15 K.

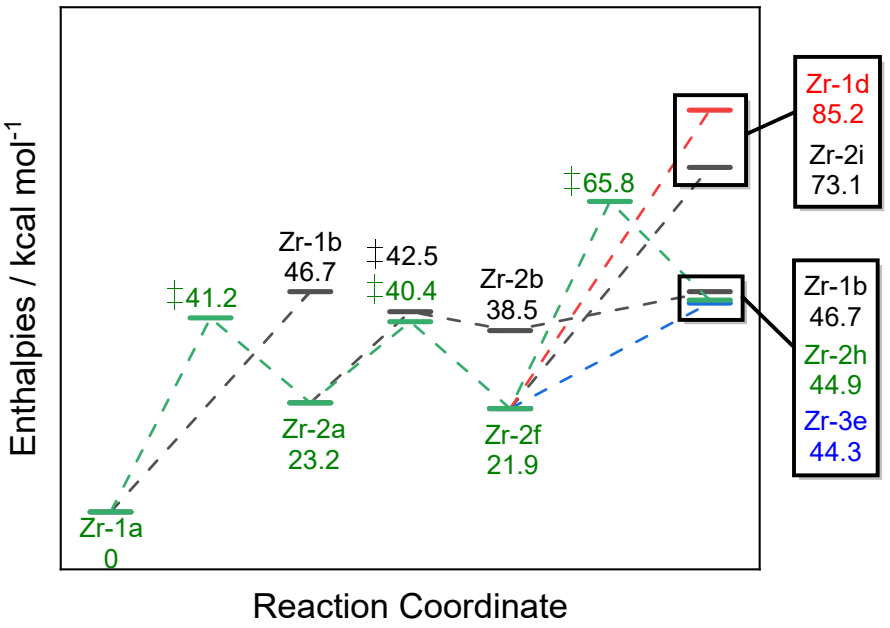

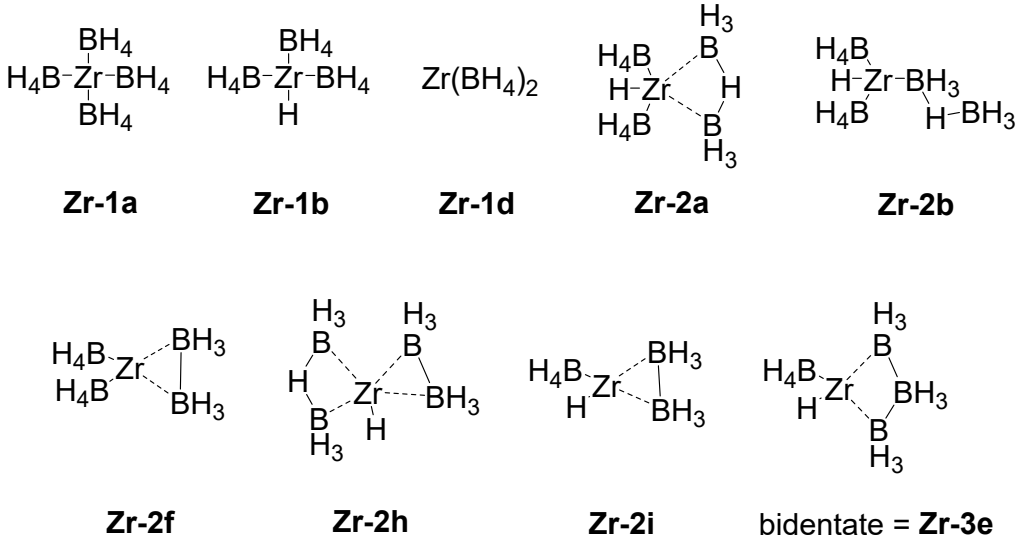

Figure S4: Reaction coordinate diagram of the low energy pathway of $Zr(BH_4)_4$ reactions. All enthalpies were calculated at 298.15 K.

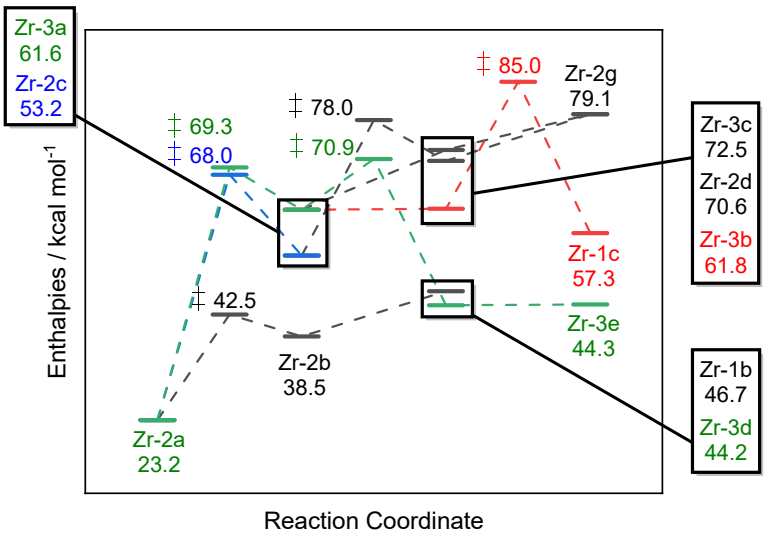

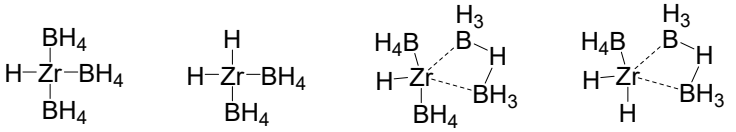

Zr-1b **Zr-1c** **Zr-2a** **Zr-2g**

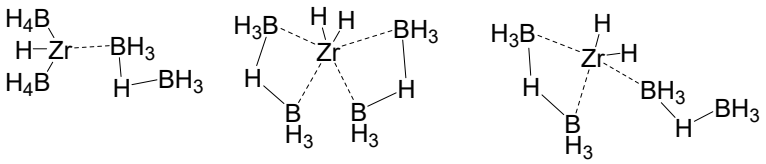

Zr-2b **Zr-2c** **Zr-2d**

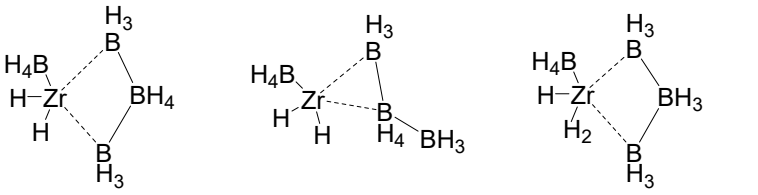

tridentate = **Zr-3a**

bidentate = **Zr-3b**

Zr-3c

tridentate = **Zr-3d**

bidentate = **Zr-3e**
(lose H_2)

Figure S5: Reaction coordinate diagram of the high energy pathway of $Zr(BH_4)_4$ reactions. All enthalpies were calculated at 298.15 K.

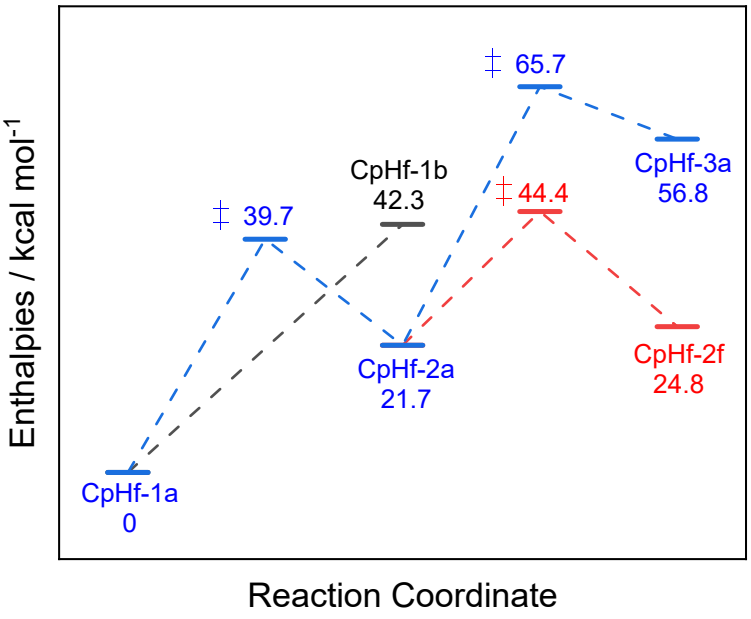

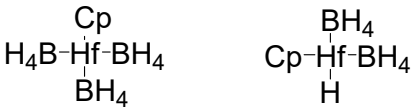

CpHf-1a

CpHf-1b

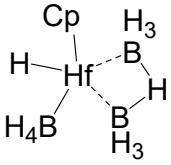

CpHf-2a

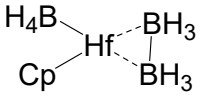

CpHf-2f

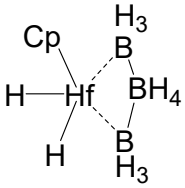

tridentate = **CpHf-3a**

Figure S6: Reaction coordinate diagram of the initial reactions of all $CpHf(BH_4)_3$ pathways. All enthalpies were calculated at 298.15 K.

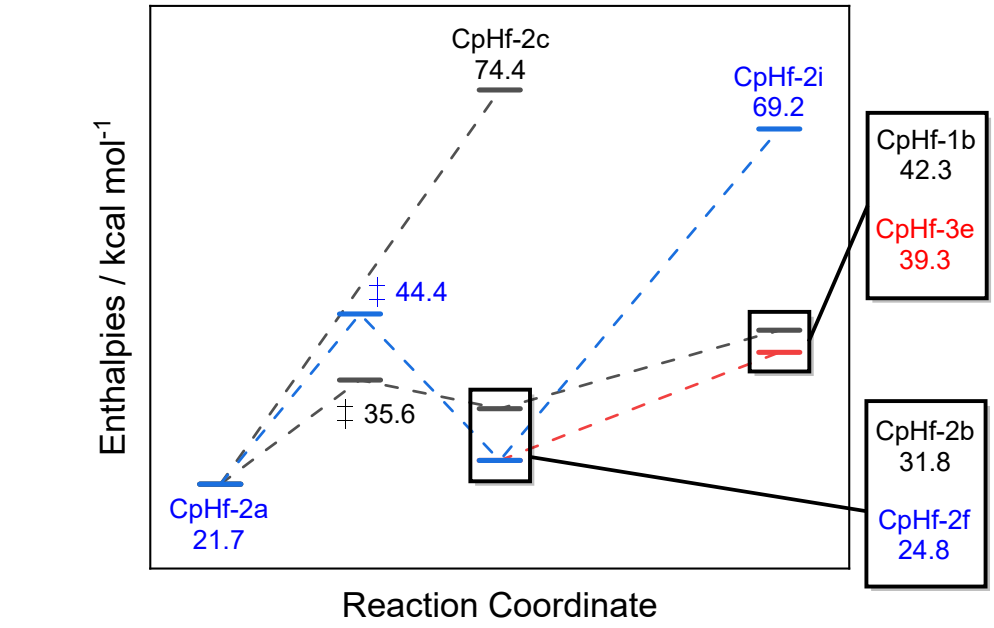

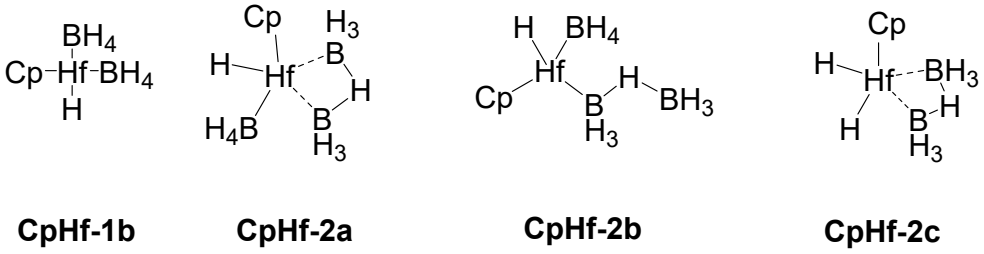

CpHf-1b **CpHf-2a** **CpHf-2b** **CpHf-2c**

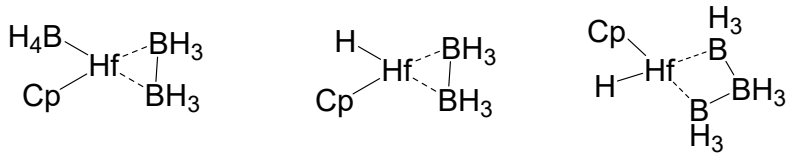

CpHf-2f **CpHf-2i** bidentate = **CpHf-3e**

Figure S7: Reaction coordinate diagram of the low energy pathway of $CpHf(BH_4)_3$ reactions. All enthalpies were calculated at 298.15 K.

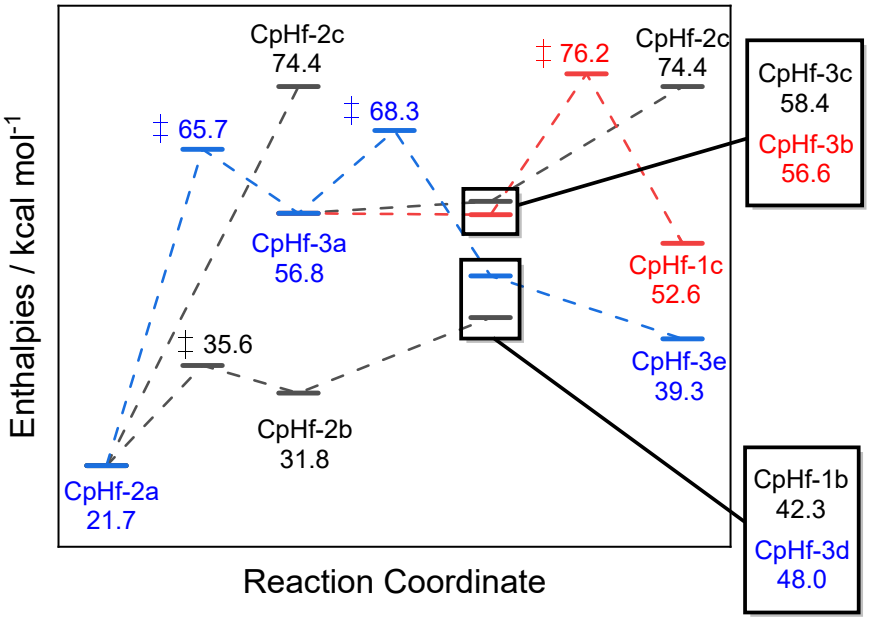

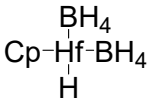

CpHf-1b

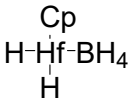

CpHf-1c

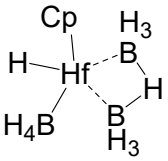

CpHf-2a

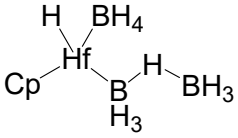

CpHf-2b

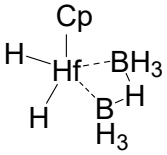

CpHf-2c

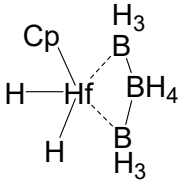

tridentate = **CpHf-3a**

bidentate = **CpHf-3b**

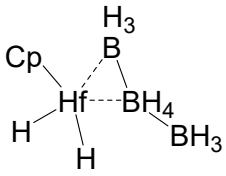

CpHf-3c

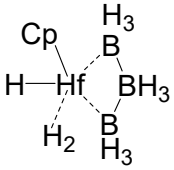

tridentate = **CpHf-3d**

bidentate = **CpHf-3e** (lose H_2)

Figure S8: Reaction coordinate diagram of the high energy pathway of $CpHf(BH_4)_3$ reactions. All enthalpies were calculated at 298.15 K.

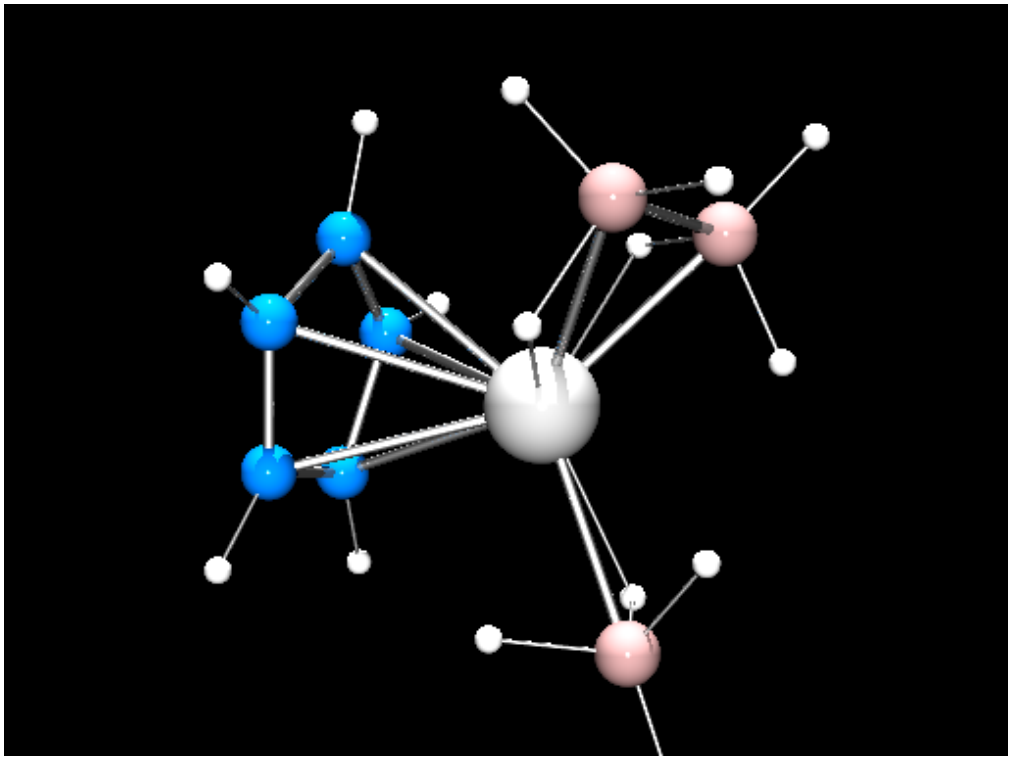

*Figure S9: Visualization of **CpHf-2f** structure - note gauche conformation of the B_2H_6 ligand.*

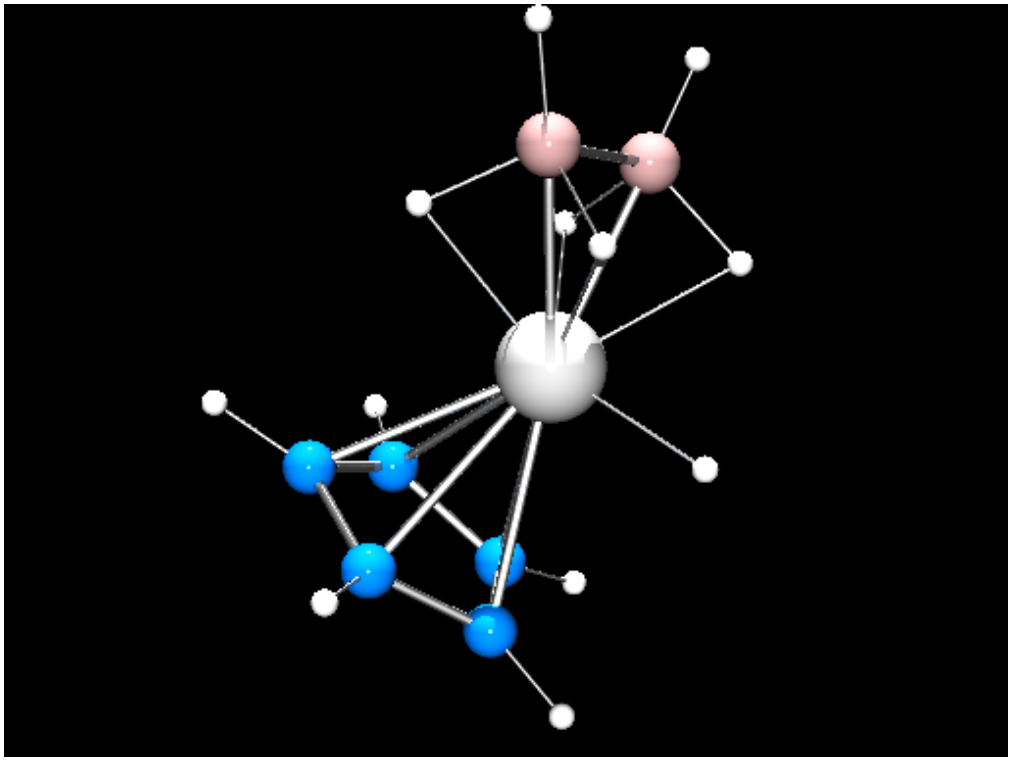

*Figure S10: Visualization of **CpHf-2i** structure. Note eclipsed conformation of B_2H_6 ligand.*

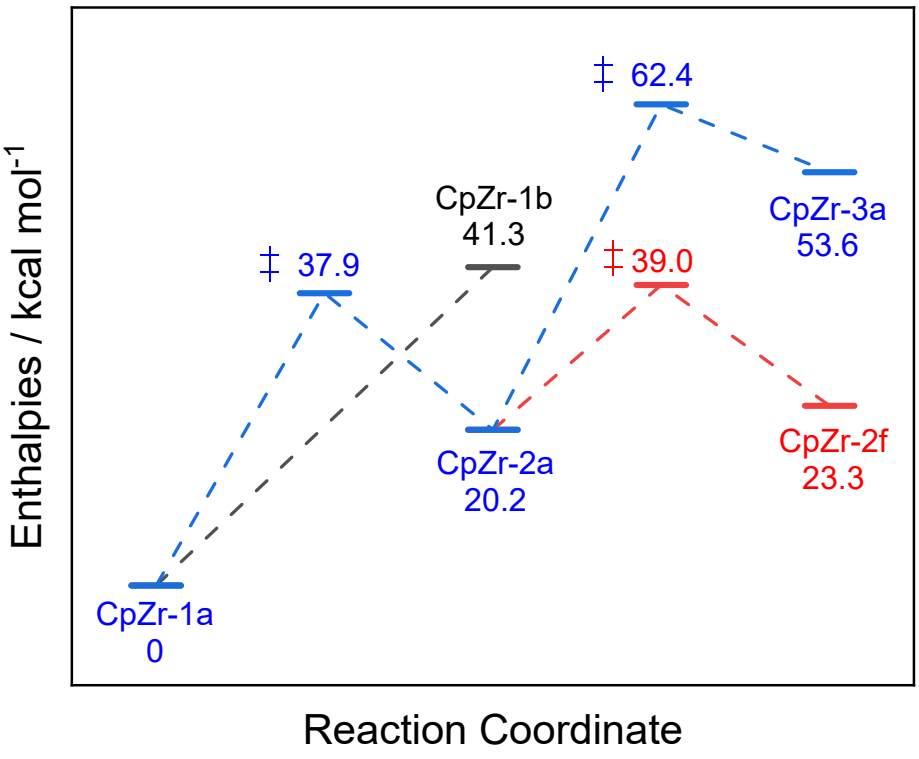

CpZr-1a

CpZr-1b

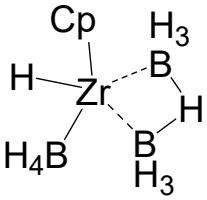

CpZr-2a

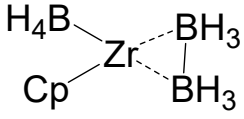

CpZr-2f

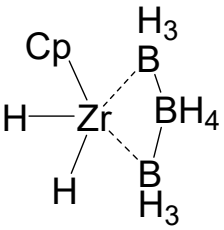

tridentate = **CpZr-3a**

Figure S11: Reaction coordinate diagram of the initial reactions of all $CpZr(BH_4)_3$ pathways. All enthalpies were calculated at 298.15 K.

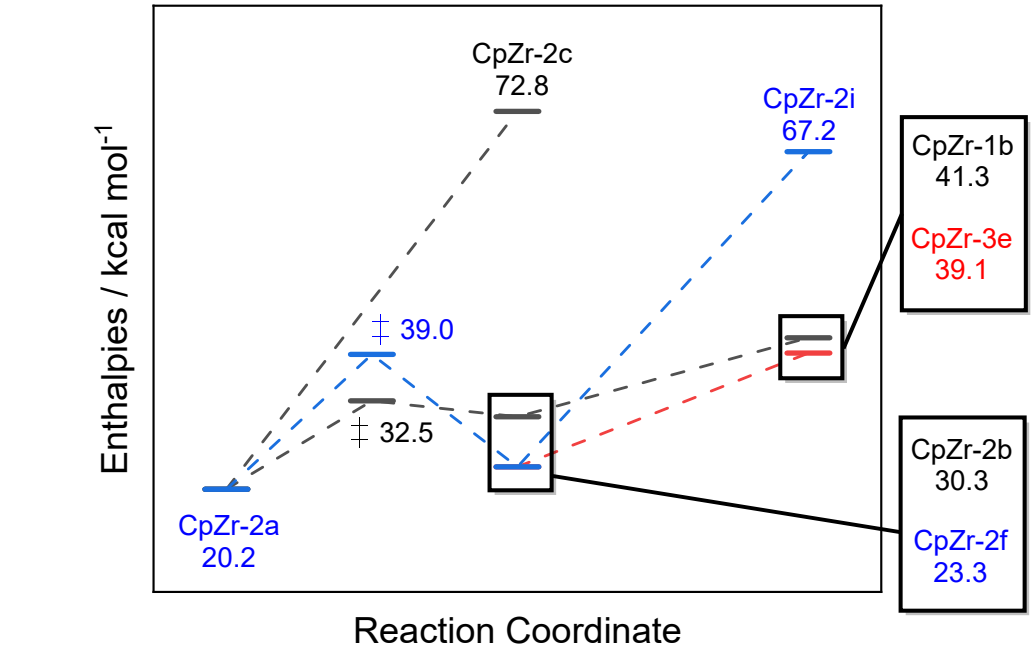

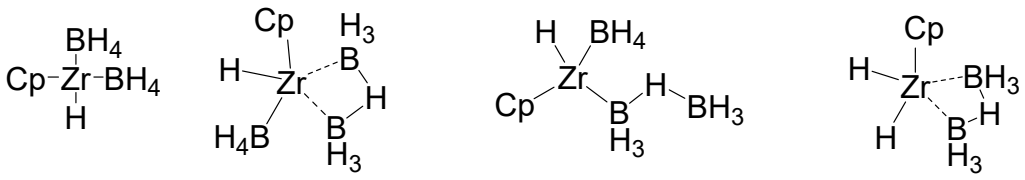

CpZr-1b **CpZr-2a** **CpZr-2b** **CpZr-2c**

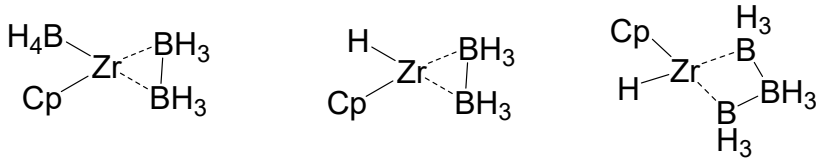

CpZr-2f **CpZr-2i** bidentate = **CpZr-3e**

Figure S12: Reaction coordinate diagram of the low energy pathway of $CpZr(BH_4)_3$ reactions. All enthalpies were calculated at 298.15 K.

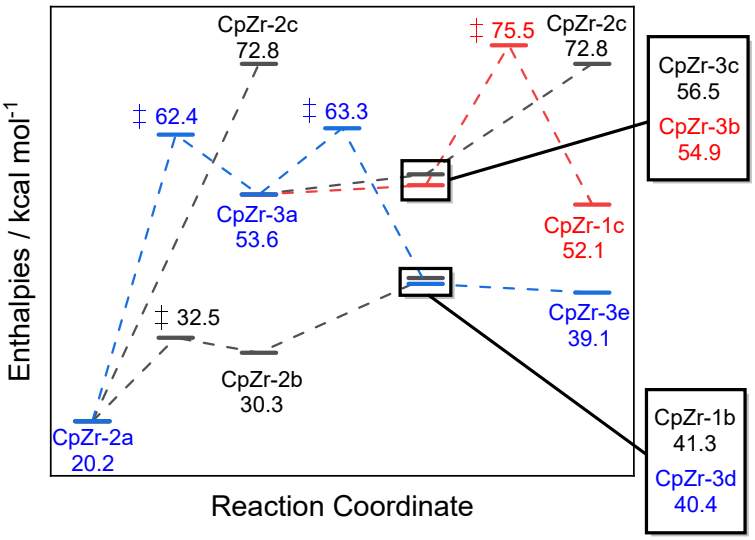

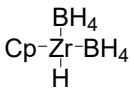

CpZr-1b

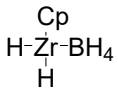

CpZr-1c

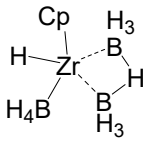

CpZr-2a

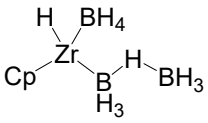

CpZr-2b

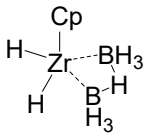

CpZr-2c

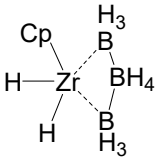

tridentate = **CpZr-3a**

bidentate = **CpZr-3b**

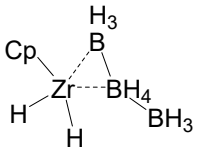

CpZr-3c

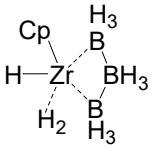

tridentate = **CpZr-3d**

bidentate = **CpZr-3e** (lose H_2)

Figure S13: Reaction coordinate diagram of the high energy pathway of $CpZr(BH_4)_3$ reactions. All enthalpies were calculated at 298.15 K.